PROGRESS IN COLOR, COLORANTS AND COATINGS

available online @ www.pccc.icrc.ac.ir

Prog. Color Colorants Coat. 14 (2021), 89-100

Ministry of Science, Research and Technology
Institute for Color Science and Technology

Removal of Methylene Blue from Water by Polyacrylonitrile-Co-Sodium Methallylsulfonate Copolymer (AN69) and Polysulfone (PSf) Synthetic Membranes

E. Cheikh S'Id[1,2*], A. Kheribech[1], M. Degué[2], Z. Hatim[1], R. Chourak[1], C. M'Bareck[2*]

[1.] Research Team: Energy, Materials and Environment (E.M.E.), FS, University of Chouaib Doukkali, P.O. Box: 20, 24000, El-Jadida, Morocco.

[2.] Research unit: Polymer, Processes and Aquatic Medium (2PMA), FST, University of Nouakchott Al-Aasriya, P.O. Box: 5026, Nouakchott, Mauritania.

ARTICLE INFO

Article history:
Received: 19 Feb 2020
Final Revised: 27 June 2020
Accepted: 28 June 2020
Available online: 16 Aug 2020

Keywords:
Methylene blue
Dye removal
AN69
Adsorption
Water treatment.

ABSTRACT

Polyacrylonitrile-co-sodium methallylsulfonate copolymer (AN69) and polysulfone (PSf) synthetic membranes were prepared and used for the removal of methylene blue (MB) from water. Atomic Force Microscopy (AFM), Ionic exchange capacity (IEC), and Swelling ratio (Sr) were employed to determine the membrane characteristics. pH, membrane composition and initial dye concentration were used for the evaluation of the efficiency of MB adsorption on AN69/PSf membranes. Isotherms and kinetic models were applied to determine the adsorption mechanism and to calculate the values of adsorption parameters. The various methods reveal that with the increase of PSf percentage, the membrane surface becomes rougher and the average values of ionic exchange capacity and the swelling ratio reach 0.6 meq/g and 7%, respectively. The adsorption of MB is more efficient at higher pH (92%) and the maximum adsorption capacity reaches 75.75 mg/g. The mechanism of adsorption is perfectly fitted by pseudo-second order (R^2 = 0.984) whereas the isotherm adsorption follows better the Freundlich isotherm (n = 1.49 and R^2 = 0.96). Prog. Color Colorants Coat. 14 (2021), 89-100© Institute for Color Science and Technology.

1. Introduction

Currently, dyes are widely used as coloring agents in several industries: leather, textiles, food, cosmetics, medicine and etc. They are belonging to the various pollutants which constitute the wastewater discharged in nature. Due to their toxicity and environment disturbance, they continue to attract great concern [1–3].

The removal of dyes from wastewater was realized by various conventional and advanced methods [2–8]. Several researches were published on the advantages and disadvantages of these methods. Membrane separation processes are commonly applied in the removal of several types of dyes [2, 9–14]. These processes are considered in much works as powerful techniques to achieve the removal of various pollutants from water and to respect the stringent regulations for wastewater disposal into environment [2, 10, 11, 15].

Methylene blue (MB) is a cationic dye. It is soluble in water and often used in textiles and food industries. Above a certain amount, the consumption of MB provokes a harmful effect on human health as high blood pressure, abdominal pain, nausea and mental

*Corresponding author: cheikhatti@gmail.com
chamec10@yahoo.com

disorder [16, 17]. Several studies were focused on the removal of MB from water [4, 8, 18–24]. In fact, this dye offers particular characteristics: a small molecular weight and positive charges. Therefore, its removal by any material opens various possibilities to remove other pollutants having comparable characteristics.

Polysulfone (PSf) is hydrophobic polymer which is usually employed to prepare membranes with high mechanical and chemical stability. To overcome the hydrophobic character, hydrophilic components were added [25–28] to improve significantly the membrane performance in the removal of dye which reaches more than 93 to 99% [10, 11, 15].

The main objective of this investigation was to synthesize ion exchange membranes with excellent mechanical and chemical properties and their application for the removal of methylene blue (MB) from water. The characteristics of AN69/PSf membranes were performed by the study of their morphology, swelling ratio, ion-exchange capacity and polymer composition. Whereas their qualities were determined by the application of isotherm and kinetic adsorption models using methylene blue (MB) as adsorbate.

2. Experimental

2.1. Materials

Poly acrylonitrile-co-sodium methallylsulfonate copolymer (AN69) was supplied by Rhodia (France), whereas polysulfone (PSf), dimethyl formamide (DMF) and methylene blue (MB) were acquired from Sigma-Aldrich Chemicals. All products were used without any purification.

2.2. Membrane preparation

Figure 1 introduces the chemical structures of polymers and dye. AN69 was dissolved in DMF solvent, with 5% (wt/v) concentration under stirring to form a dope solution. The PSf was added in known proportions and the mixtures were stirred for 3 hours, de-bubbled and casted on a glass plate with a laboratory-made Gardner knife. The cast liquid film was died in oven at 80 °C for 30 minutes, and finally immersed in a coagulation bath containing a sufficient volume of MilliQ water at 24 °C. The membranes were thoroughly washed with water and stored until their use.

2.3. Ion exchange capacity measurement

The ion exchange process takes place without substantial modification of membrane structure. The ion exchange capacity was determined after alternative sample conditionings in 0.1 M NaOH and 0.1 M HCl for an immersion time for 4 hours. In H^+ form, the sample was equilibrated in water for 12 hours to remove the free hydrogen ions and afterwards immersed in NaCl 0.1M for 4 hours. The released H^+ ions in the NaCl medium were titrated by NaOH 0.01M [26, 29].

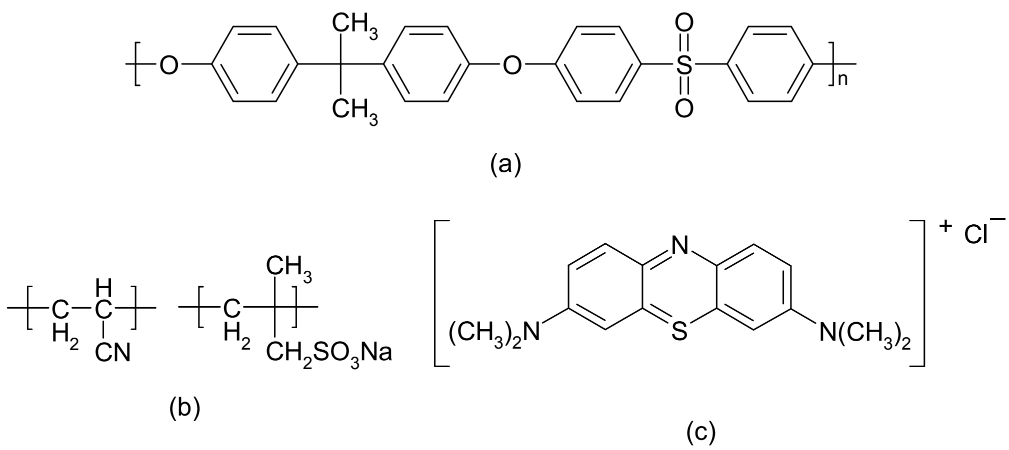

Figure 1: Structures of PSf (a), AN69 (b) and MB dye (c).

2.4. Swelling ratio

The water content of the membranes was calculated from the weight difference between the swollen-membrane weight (W_{sw}) and the dried-membrane weight (W_{dr}). The swelling ratio is usually determined to get an idea of the extension of membrane structure. The swelling ratio (S_r) is calculated by the following formula (Eq. 1):

$$Sr = \frac{W_{ws} - W_{dr}}{W_{ws}} \quad (1)$$

2.5. Atomic force microscopy (AFM)

The membranes surfaces were analyzed by a "Nanoscope II" from Digital Instruments™ (Santa Barbara, USA) using a 140-µm scanner. The cantilevers used were characterized by a spring constant of 0.06 N/m. A standard pyramidal tip in silicon nitride was used.

2.6. Adsorption of methylene blue

Using 50 mL Erlenmeyer flasks, a batch adsorption experiments were carried out at ambient temperature 298 K. The Erlenmeyer flasks containing membrane samples were agitated at constant speed of 120 T/min for a known time. The range concentration of dye was between 10 and 40 ppm. The effects of membrane composition, dye concentration and pH were investigated.

The dye absorption was measured at the wavelength corresponding to the maximum absorption, λ_{max}= 663 nm, using 6705 UV/Vis. Spectrophotometer, model JENWAY. The amount of dye adsorbed onto membrane Q_e (mg/g) was calculated using Equation 2:

$$Q_e = \frac{(C_0 - C_e)\,V}{m} \quad (2)$$

Where Q_e is the adsorbent amount of dye (mg/g); C_0 (mg/L) and C_e (mg/L) are the initial and equilibrium concentrations of dye, respectively; m (g) is the mass of membrane sample (10 mg); and V (L) is the volume of the liquid phase (25 mL).

The Adsorption efficiency or dye retention (R) is calculated by using Equation 3:

$$R\ \% = \frac{C_0 - C_e}{C_0} \times 100 \quad (3)$$

3. Results and Discussion

3.1. Ion exchange capacity (IEC) and swelling ratio (Sr)

The determination of IEC and Sr is useful to understand the mechanism on intermolecular interactions between membrane and pollutants and the physical extension of membrane in aqueous solution. Then, three samples, AN69/PSf 95/05, 90/10 and 86/14 membranes were used to measure the ionic exchange capacity and the swelling ratio as summarized in Table 1.

The results show that the decrease of IEC and Sr values is associated to a decrease of AN69 percentage. In fact, this trend is due to the decrease of hydrophilic groups (SO_3^-) embedded in AN69 copolymer and the increase of PSf percentage which is a hydrophobic polymer [27, 29]. The presence of ionic charges (SO_3^-) has a benefit factor in the removal of pollutants and the increase of permeability and antifouling performance [30]. It should be noted that the roughness of the membrane surface increases with the increase of PSf percentage as observed with the naked eye. This trend was assigned to the retraction of PSf chains under the forces of non-solvent penetration (water) [31].

Table 1: Membrane trends, Swelling Rate (Sr) and Ion Exchange Capacity (IEC).

Membrane composition	Surface features	IEC (meq/g)	Sr %
AN69/PSf 95/05	almost smooth	0.61	8.14
AN69/PSf 90/10	Slightly rough	0.57	7.3
AN69/PSf 86/14	Rough	-	5.27

3.2. Atomic Force Microscopy (AFM)

Atomic Force Microscopy (AFM) was used to determine the membrane topography which can impact the results of kinetic and isotherm adsorption. AN69/PSf 95/05 and 90/10 membranes were used to study the effect of polymer proportion on the topography of membrane surface as displayed by Figure 2.

From the comparison of the features of the both samples, it was observed that the roughness of the surface increases with the augmentation of PSf percentage. The surface of AN69/PSf 95/05 membrane is smoother than that of AN69/PSf 90/10 which presents important reliefs [28, 32, 33] observed also by the naked eye. Otherwise, the appearance of very small pore structures with different sizes becomes more noticeable in AN69/PSf 90/10 membrane. The change in membrane morphology with the increase of PSf is certainly due to the dimixing process which is governed by the forces of solvent exclusion and non-solvent penetration [26, 31].

3.3. Methylene blue adsorption

In Adsorption experiences, 10mg of membrane was immersed in 25 mL under 120 rpm at 298 K and pH 10.8.

3.4. Effect of pH solution

Figure 3 introduces the variation of adsorption retention as a function of initial pH of dye solution. It appears that the retention of MB improves significantly with the pH increase. It improves from 61% at pH 3.8 to 92% at pH 10.8.

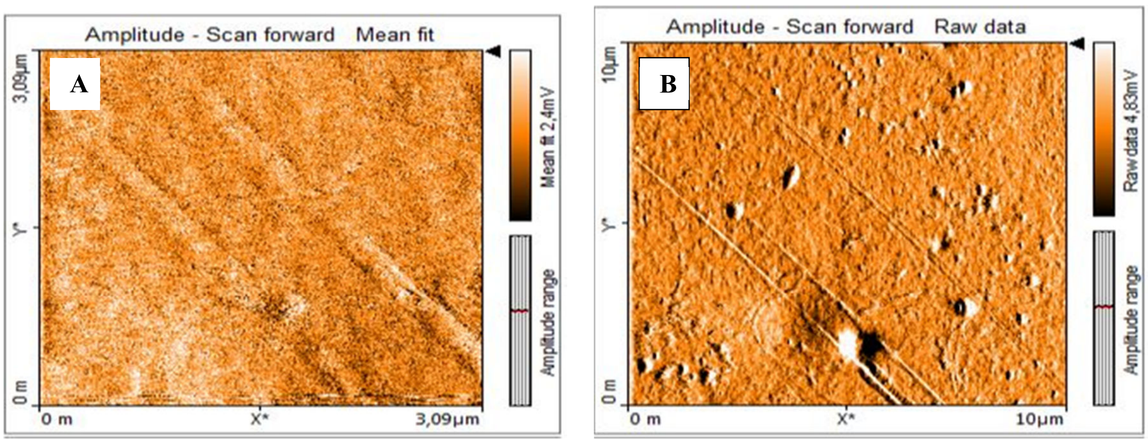

Figure 2: AFM images of (a) AN69/PSf 95/05 and (b) AN69/PSf 90/10 membrane surfaces.

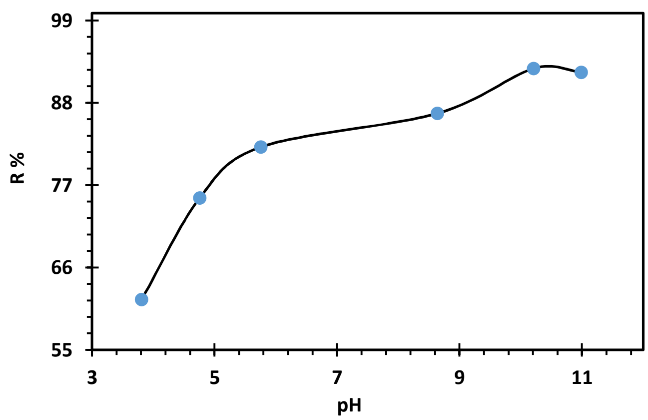

Figure 3: Effect of pH on MB adsorption on PSf/PAA 90/10 membrane at C_{dye} = 15 mg/L.

AN69/PSf membranes contain negative charges ($-SO_3^-$) which might be considered as strong electrolyte whereas MB molecules contain positive charges. The ionization of dye molecules depends on pH. Thus, the increase in pH enhances the ionization of all groups embedded in the both polymers and improves the intermolecular interactions among their segments (adsorption) [29]. E. Makhado et al. has attributed the high adsorption of MB on hydrogel grafted- poly acrylic acid to the strong intermolecular interactions between dye (MB) and membrane. These interactions involved the positive charges within MB molecules and the negative charges of poly/acrylic acid embedded in grafted hydrogel [34]. Therefore, all the following experiments will be done at constant pH 10.8 in order to improve the efficiency of MB adsorption on AN69/PSf membranes.

3.5. Effect of membrane composition

AN69/PSf 95/05, 90/10 and 86/14 membranes were tested in order to discover the impact of membrane composition on adsorption of MB as illustrated by Figure 4.

The different curves show an increase of MB retention with the increase of AN69 percentage. The equilibrium adsorption capacity reached 98.43, 76.39 and 62.22 mg/g for AN69/PSf 95/05, 90/10 and 86/14 membrane, respectively. It should be noted that AN69/PSf 95/05 offers the best results due to the high ion exchange capacity and the swelling ratio mentioned above. Both parameters play an important role in the improvement of intermolecular interactions between dye and membrane charges, in the one side, and the penetration of dye molecules into membrane structure, in the other side.

The decrease of adsorption capacity with the increase of PSf percentage confirms that the adsorption is mainly due to the establishment of interactions between positive charges embedded in dye molecules and negative charges supported by AN69 copolymer [35]. Similar results were noted by many researchers who assigned the adsorption of different cationic dyes on negative charged polyelectrolyte to the establishment of attractive electrostatic interactions between their segments [29, 36, 37].

3.5.1. Effect of initial concentration of MB

Due to its highest ion exchange capacity AN69/PSf 95/05, membrane was used to verify the effect of initial concentration on MB adsorption. Figure 5 represents the different curves obtained at different concentrations 10, 25 and 35 mg/L. In the light of these results, it seems clear that both equilibrium adsorption capacity and equilibrium time increase with the augmentation of dye concentration. Therefore, the adsorption improves with the initial concentration increase [37, 38]. In fact, the increase of the concentration provokes an increase of dye density in the surroundings of the functional sites embedded in AN69/PSf membrane where the reorganization of dye molecules need longer time [29, 39]. This behavior might be taken as a sign of the dominance of physical interactions between dye charges and membrane functional sites in agreement with the Freundlich theory [40].

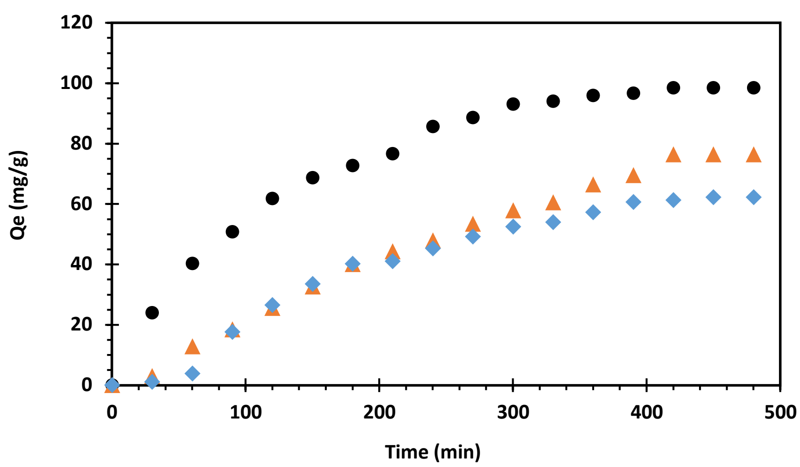

Figure 4: Effect of membrane composition: AN69/PSf 95/05 (●), AN69/PSf90/10 (▲) and AN69/PSf 86/14 (◆).

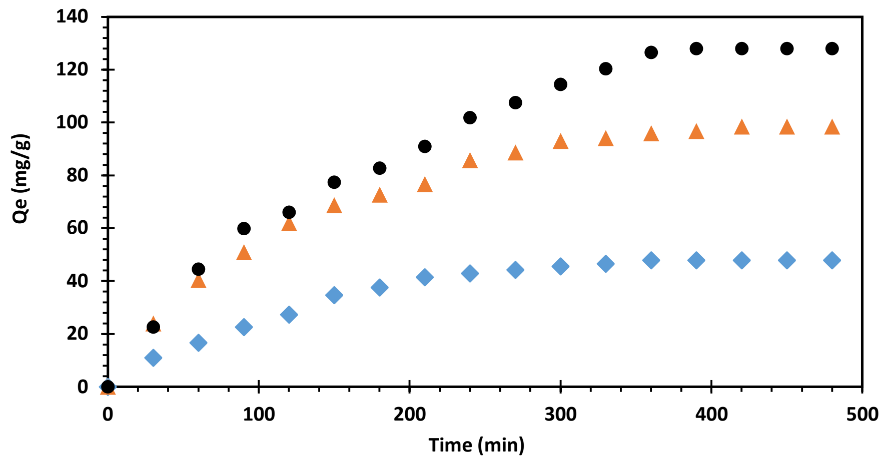

Figure 5: Effect of dye concentration: (◆) 10, (▲) 25 and (●) 35 mg/L.

3.5.2. Kinetic Study

The kinetic measurements was limited to the most used models in literature: pseudo first order and pseudo second order [41].

Pseudo first order model: the linear form of pseudo first order is given by the Equation 4:

$$\text{Ln}\,(q_e - q_t) = \text{Ln}\,q_e - K_1\,t \text{ [42]} \tag{4}$$

Where q_t and q_e are the capacities of adsorption at instant t and equilibrium time, respectively. K_1: is the equilibrium rate constant (min^{-1}).

Table 2 summarizes the values of kinetic adsorption parameters of MB adsorption deduced from Figure 6, which illustrates the Pseudo-first-order model at different concentrations. Table 2 shows that with the increase of MB concentration, the equilibrium adsorption capacity increases; and the difference between the value of correlation constant and unit (1) increases significantly. The decrease of the correlation coefficient with the increase of the concentration reveals that Pseudo first order model is not suitable to describe the mechanism of MB adsorption on AN69/PSf membrane.

Pseudo second order model: the linear form of pseudo second order as proposed by McKay and Ho is given by the following equation (Eq. 5)

$$\frac{t}{q_t} = \frac{1}{(K_2 \cdot q_e^2)} + \frac{t}{q_e} \tag{5}$$

Where q_t and q_e are the adsorption capacities at instant t and equilibrium time, respectively, K_2: is the equilibrium rate constant of the second pseudo order (g min / mg).

The plot of t/q_e versus t is illustrated by Figure 7. Table 3 summarizes the values of kinetic parameters deduced from Figure 7 which illustrated the application of pseudo second kinetic model [41].

Table 2: Values of equilibrium adsorption capacity q_e, adsorption constant K_1 and the correlation coefficient R^2, according to Pseudo-first-order model, at different concentrations of MB solutions.

		Pseudo-first order		
C_0 (mg/L)	$Q_{e,\,exp}$ (mg/g)	$Q_{e,\,cal}$ (mg/g)	K_1 (min^{-1})	R^2
10	47.86	59.02	1.06 10^{-2}	0.983
25	98.43	120.72	1.01 10^{-2}	0.973
35	127.96	179.7	0.96 10^{-2}	0.851

Table 3: Values of equilibrium adsorption capacity q_e, adsorption constant K_2 and the correlation coefficient R^2, according to Pseudo-second-order model, at different concentrations of MB solutions.

		Pseudo-second order		
C_0 (mg/L)	$Q_{e.\ exp}$ (mg/g)	$Q_{e.\ cal}$ (mg/g)	K_2 (g min / mg)	R^2
10	47.86	65.78	$1.02\ 10^{-4}$	0.982
25	98.43	128.2	$5.99\ 10^{-5}$	0.996
35	127.96	192.3	$2.39\ 10^{-5}$	0.986

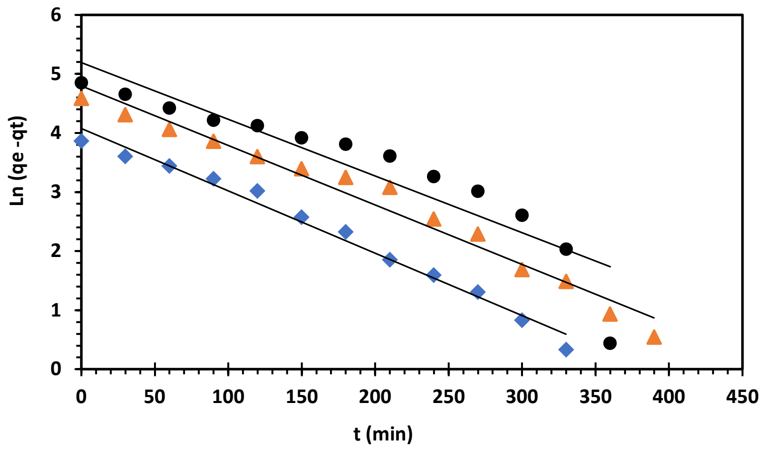

Figure 6: Pseudo first order kinetic curves for the MB adsorption on AN69/PSf 95/05 membrane at C_0 = 10 (◆), 25 (▲) and 35 mg/L (●).

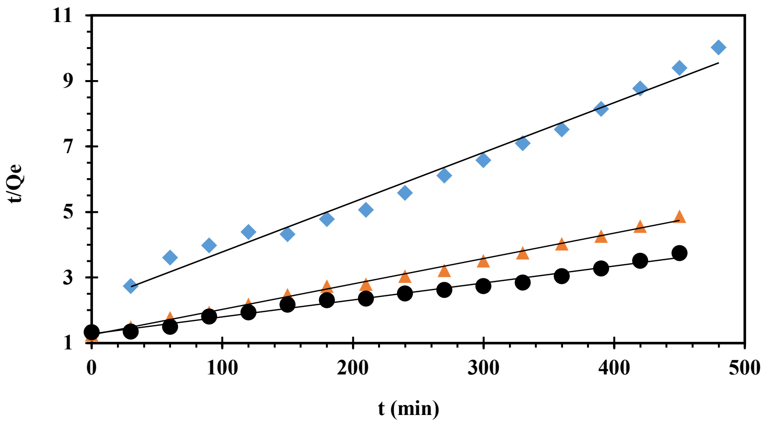

Figure 7: Pseudo second order kinetic curves for the MB adsorption on AN69/PSf membrane at C_0 = 10 (◆), 25 (▲) and 35 mg/L (●).

In spite of the difference between the values of experimental and theoretical capacities, the change of correlation coefficient is very weak regardless of the concentration of MB solution. These results confirm that the mechanism of MB adsorption on AN69/PSf membrane obeys preferentially to the pseudo-second-order model which governs the intermolecular interactions between dye molecules and adsorbents. The obtained values of pseudo second order constants of the MB adsorption onto AN69/PSf membranes, summarized in Table 4, are comparable with those of the adsorption of MB on various membrane and bio-adsorbent materials as: cotton stalk [7] hawthorn kernel and Sulphonated Hawthorn kernel [16], citrus limetta peel waste [19], modified wheat straw [20], parsley stalk [21], rice hull ash [22], shaddock peel [23], zein/graphene oxide nanofibrous composite [24], Seed powder of Punicagranatum [43], cellulose acetate nanofibrous membranes modified by polydopamine [44], onion membranes [45] and poly (L-lactic acid) electrospun nanofiber membrane [46].

3.5.3. Adsorption isotherms

The most used models for isotherms adsorption were applied to determine the maximum adsorption capacity of MB and the isotherm constants.

a) Langmuir's model

According to Langmuir hypothesis [47], the deposition of adsorbate molecules (MB) on the adsorbent surface (AN69/PSf membrane) might be described by the following mathematical equation (Eq. 6):

$$Q_e = \frac{Q_m \cdot K_L \cdot C_e}{1 + K_L \cdot C_e} \qquad (6)$$

Where Q_e is the amount of MB adsorbed per gram of the adsorbent at equilibrium (mg/g), C_e is the equilibrium concentration of adsorbate (mg/L), Q_m is the maximum monolayer coverage capacity (mg/g) and K_L is Langmuir isotherm constant (L/mg).

The linearization of this equation leads to the following equation (Eq. 7):

$$\frac{1}{Q_e} = \frac{1}{Q_m} + \frac{1}{K_L \cdot Q_m \cdot C_e} \qquad (7)$$

So, the plot of 1/ Q_m versus 1/C_e as shown in Figure 8, is employed to deduce the values of Q_m and K_L. The Langmuir isotherm constant might be used to calculate the Langmuir separation factor R_L from the following Equation (8):

$$R_L = \frac{1}{1+K_L \cdot C_0} \qquad (8)$$

It should be noted that the adsorption is considered favorable when R_L is between 0 and 1, linear if $R_L = 0$ and, not favorable when the R_L values are greater than 1 [48].

Table 4: Pseudo- second order constants for the adsorption of MB onto various membranes and bio-adsorbents.

Adsorbent	Pseudo second order constants		Correlation constant	Reference
	Q_{cal} (mg/g)	K_2 (g/mg·min)	R^2	
Cotton Stalk	104.82	0.00519	0.999	[7]
Hawthorn kernel	28.25	2.44	0.999	[16]
Sulphonated hawthorn kernel	51.28	1.57	0.994	[16]
Citrus limetta peel waste	23.25	0.057	0.99	[19]
Modified wheat straw	217.4	0.1722	0.997	[20]
Rice hull ash	48.10	0.069	1.00	[22]
Shaddock peel	124.55	0.00006	0.999	[23]
Seed powder of Punicagranatum	28.735	0.022	0.999	[43]
Polyacrylonitrile-co-sodium methallylsulfonate copolymer (AN69) and polysulfone (PSf) synthetic membranes	192.3	0.0000239	0.986	This study
Cellulose Acetate Nanofibrous Membranes Modified by Polydopamine	96.9	0.000117	0.999	[44]
Onion membrane	1.316	0.000002	0.989	[45]
Poly (L-lactic acid) electrospun nanofiber membrane	1.1017	1.2813	0.999	[46]

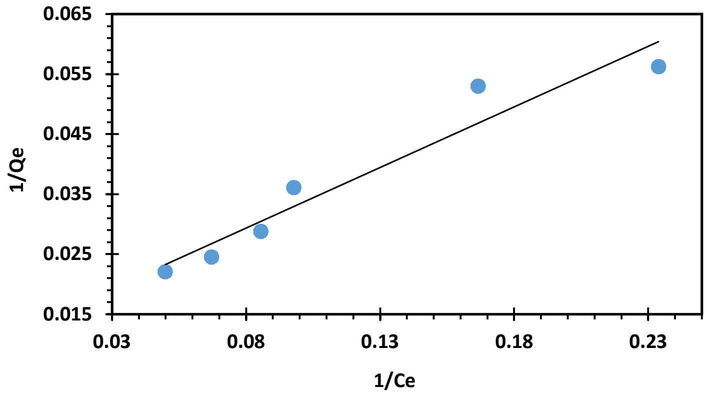

Figure 2: Langmuir model for AN69/PSf 95/05 membrane at C_0 = 10 to 40 mg/L.

The plot of Langmuir model permits the deduction of maximum adsorption capacity (Q_m = 75.75 mg/g), the correlation coefficient (R^2 = 0.93), the Langmuir adsorption constant (K_L = 0.064 L/mg) and the separation factor R_L with values ranging between 0.28 and 0.6. In spite of the divergence between the values of correlation coefficient and 1, all values of separation factor are including in the interval 0 and 1. Then, based on the values of separation factor, the adsorption of MB onto AN69/PSf membrane is favorable.

b) Freundlich's model

Freundlich [40] proposed an experimental model to describe the adsorption phenomenon. This model is interpreted by the following equation:

$$Q_e = K_f\, C_e^{1/n} \tag{9}$$

Where Q_e is the amount of dye adsorbed per gram of the adsorbent at equilibrium (mg/g), C_e is the equilibrium concentration of adsorbate (mg/L), K_f is the adsorption capacity at unit concentration and 1/n is the adsorption intensity. Freundlich's parameters can be deduced from the linearization of the above equation:

$$\text{Ln Qe} = \text{LnK}_F + \frac{1}{n}\,\text{Ln Ce} \tag{10}$$

The value of Freundlich intensity (n) as deduced from Figure 9 was 1.49 and that of correlation coefficient (R^2) was 0.962. They confirm that the adsorption of MB is fitted better by Freundlich model than Langmuir [48]. Therefore, it might be admitted that the reorganization of dye molecules in the surrounding of membrane functional sites follows preferentially the Freundlich model approach.

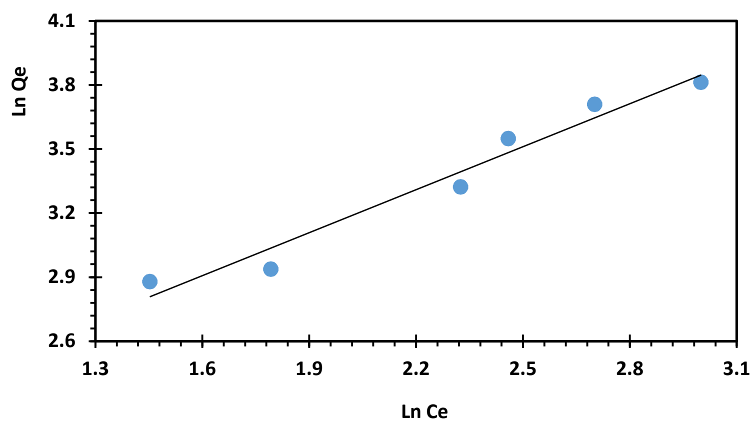

Figure 9: Freundlich model for AN69/PSf 95/05 membrane at C_0 = 10 - 40 mg/L.

Table 5: Values of adsorption parameters from Langmuir and Freundlich models.

Langmuir				Freundlich		
R^2	Q_m(mg/g)	K_L(L/mg)	R_L	R^2	n	K_F (mg/g) (L/mg)$^{1/n}$
0.93	75.75	0.064	0.28 and 0.6	0.962	1.49	6.24

Table 6: Langmuir isotherm parameters for the adsorption of MB on various membranes and bio-adsorbents.

Adsorbent	Langmuir constant		Correlation constant	Reference
	Q_m(mg/g)	K_L (L/mg)	R^2	
Cotton Stalk	147.1	0.0249	0.997	[7]
Hawthorn kernel	43.7	0.037	0.9408	[16]
Sulphonated Hawthorn kernel	151.5	5.50	0.5696	[16]
Citrus limetta peel waste	227 .3	0.0289	0.9787	[19]
Modified wheat straw	216.9	51.05	0.999	[20]
Rice hull ash	17.1	0.606	0.998	[22]
Shaddock peel	309.6	0.0146	0.999	[23]
Seed powder of Punicagranatum	99.009	0.034	0.991	[43]
Polyacrylonitrile-co-sodium methallylsulfonate copolymer (AN69) and polysulfone (PSf) synthetic membranes	75.75	0.064	0.93	This study
Cellulose Acetate Nanofibrous Membranes Modified by Polydopamine	165.837	2.046	0.993	[44]
Onion membrane	1.905	72.38	0.987	[45]
Poly (L-lactic acid) electrospun nanofiber membrane	8.7306	0.2584	0.993	[46]

The adsorption parameters determined from both models, illustrated by Table 5, show that the adsorption of MB on AN69/PSf is favorable, and it seems to be in total conformity with Freundlich model which suggests the heterogeneity of membrane surface as shown by topographic investigation (AFM) as proposed previously.

In fact, based on the different results (Q_m = 75.75 mg/g, n = 1.49, R^2 = 0.96), it might be noted that the rate of intermolecular interactions between dye molecules and membrane is not strong enough to allow a high adsorption rate of MB on AN69/PSf membrane. The adsorption is preferentially due to the physical interactions as proposed by Freundlich model [40].

Nevertheless, the maximum monolayer adsorption capacity of MB onto AN69/PSf membrane provided an encouraging result when compared with those of adsorption of MB on various membrane and bio-adsorbent materials (agricultural by- products) as summarized in Table 6.

4. Conclusion

Novel synthetic membranescomposed of polyacrylo-nitrile-co-sodium methallylsulfonate copolymer (AN69) and polysufone (PSf) blends were prepared for the removal of methylene blue (MB) from aqueous solution. Atomic Force Microscopy was used in the morphological study, andion exchange capacity (IEC) and swellingratio (Sr) were usedin the evaluation of membranes exchange abilities. Moreover, based on the results of adsorption models, it was found that the removal of Methylene blue is due to intermolecular interactions between negative membrane charges (sulfonate groups) and positive dye molecules.

Acknowledgments

This work was done at the University of Nouakchott Al-Aasriya (Mauritania) and Chouab Doukkali University in Morocco. So, we would like to thank these universities for their support. And special thanks for Pr. Mifdal Mohamed from UCD and Mr. Mohamed Yarba Meissara.

5. References

1. M. M. Hassan, C. M. Carr, A critical review on recent advancements of the removal of reactive dyes from dye house effluent by ion-exchange adsorbents, *Chemosphere*., 209(2018), 201-219.
2. M. Gholami, S. Nasseri, M.R. Alizadehfard, A. Mesdaghinia, Textile dye Removal by membrane technology and biological oxidation, *Water Qual. Res. J. Canada.*, 38(2003), 379-391.
3. F. Mashkoor, A. Nasar, Magsorbents : Potential candidates in wastewater treatment technology – A review on the removal of methylene blue dye, *J. Magn. Magn. Mater*. 500(2020) 166408.
4. Y. Yao, F. Xu, M. Chen, Z. Xu, Z. Zhu, Adsorption behavior of methylene blue on carbon nanotubes, *Bioresour. Technol*., 101(2010), 3040-3046.
5. Q. Liu, B. Yang, L. Zhang, R. Huang, Adsorption of an anionic azo dye by cross-linked chitosan/bentonite composite, *Int. J. Biol. Macromol*., 72(2015) 1129-1135.
6. A. Aichour, H. Zaghouane-Boudiaf, C.V. Iborra, M.S. Polo, Bioadsorbent beads prepared from activated biomass/alginate for enhanced removal of cationic dye from water medium: Kinetics, equilibrium and thermodynamic studies, *J. Mol. Liq*., 256(2018) 533-540.
7. H. Deng, J. Lu, G. Li, G. Zhang, X. Wang, Adsorption of methylene blue on adsorbent materials produced from cotton stalk, *Chem. Eng. J*., 172(2011) 326-334.
8. S. Shakoor, A. Nasar, Utilization of Punica granatum peel as an eco-friendly biosorbent for the removal of methylene blue dye from aqueous solution, *J. Appl. Biotechnol. Bioeng*., 5(2018) 242-249.
9. D. M. Al-Ani, F.H. Al-Ani, Q.F. Alsalhy, S.S. Ibrahim, Preparation and characterization of ultrafiltration membranes from PPSU-PES polymer blend for dye removal, *Chem. Eng. Commun*., 32(2019), 77-86.
10. C. N. Jose Carlos C, Humberto G, Color and COD retention by nanofiltration membranes, *Desalination*., 172(2005), 77-83.
11. A. A. M. Bu-Ali Q, Haji S, Al-Bastaki N, Removal of acid red and sodium chloride mixture from aqueous solutions using nanofiltration, *Desalination*., 206(2007), 407–413.
12. T. L. Simms KM, Zaidi SA, Selection of ultrafiltration/nanofiltration membranes for treatment of textile dyeing wastewater, *Water Treat*., 9(1994), 189–198.
13. O. M. Okhuma N, Decoloration system using rotating membrane UF module, *Water Sci. Technol*., 38(1998), 635–643.
14. D. Karisma, G. Febrianto, D. Mangindaan, Removal of dyes from textile wastewater by using nanofiltration polyetherimide membrane, IOP Conf. Ser. *Earth Environ. Sci*., 109(2017), 012012.
15. A. Poulios I, Sotiriou D, Pappas M, Moutesidis K, S A, Simulated cotton dye effluents treatment and reuse by nanofiltration, *Desalination*., 221(2008), 259-267.
16. Y. Akkoz, R. Coskum, A. Delibas, Preparation and characterization of sulphonated bio-adsorbent from waste hawthorn kernel for dye (MB) removal, *J. Mol. Liq*., 287(2019), 110988.
17. W. Chai, H. Wang, Y. Zhang, G. Ding, Preparation of polydopamine-coated magnetic nanoparticles for dispersive solid-phase extraction of water-soluble synthetic colorants in beverage samples with HPLC analysis, *Talanta*., 149(2016), 13–20.
18. S. Shakoor, A. Nasar, Adsorptive treatment of hazardous methylene blue dye from artificially contaminated water using Cucumis sativus peel waste as a low-cost adsorbent, *Groundw. Sustain. Dev*., 5(2017), 152-159.
19. S. Shakoor, A. Nasar, Removal of methylene blue dye from artificially contaminated water using citrus limetta peel waste as a very low cost adsorbent, *J. Taiwan Inst. Chem. Eng*., 66(2016), 154-163.
20. Z. W. Yan H, Li H, Jiang Z, Dong L, Kan X, et al., Removal of dyes from aqueous solutions by straw based adsorbents: Batch and column studies, *Chem. Eng. J*., 168(2011), 1120-7.
21. A. G. Guzel F, Application of some domestic wastes as new low-cost biosorbents for removal of methylene blue: kinetic and equilibrium studies, *Chem. Eng. Commun*., 201(2014), 557–78.
22. C. X. Lv S, Liu S, Zhang P, Zhang A, Sun J, et al., Adsorption of methylene blue by rice hull ash, *Sep. Sci .Technol*., 47(2012), 147–56.
23. L. J. Wu J, Li P, Wang X, Yang B, Shaddock peel as a novel low-cost adsor- bent for removal of methylene blue from dye wastewater, *Desalin. Water Treat*., 39(2012), 70-75.
24. A. Soraya, S.M. Seyedahmadian, B. Habibi, K. Farhadi, An electrospun zein / graphene oxide nanofibrous composite : Typical application as a new biopolymeric adsorbent in removal of methylene blue and malachite green dyes from aqueous media, *Prog. Color Colorant Coat*., 14 (2021), xx–xxx.
25. D. Song, J. Xu, Y. Fu, L. Xu, B. Shan, Polysulfone/sulfonated polysulfone alloy membranes with an improved performance in processing

mariculture wastewater, *Chem. Eng. J*., 304(2016), 882-889.

26. C. Mbareck, Q. Trong Nguyen, O. Tahiri Alaoui, D. Barillier, Elaboration , characterization and application of polysulfone and polyacrylic acid blends as ultrafiltration membranes for removal of some heavy metals from water, *J. Hazard. Mater*., 171(2009), 93–101.
27. A. Ouradi, Q. T. Nguyen, A. Benaboura, Polysulfone-AN69 blend membranes and its surface modification by polyelectrolyte layer deposit-Preparation and characterization, *J. Memb. Sci*., 454(2014), 20-35.
28. A. T. Kuvarega, N. Khumalo, D. Dlamini, B.B. Mamba, Polysulfone/N,Pd co-doped TiO_2 composite membranes for photocatalytic dye degradation, *Sep. Purif. Technol*., 191(2018), 122-133.
29. C. M'Bareck, E. C. S'Id, A. Kheribech, A. Elouahli, Z. Hatim, Synthesis of polyacrylonitrile-co-sodium methallyl sulfonate copolymer (AN69) and polyacrylic acid (PAA) membranes for the removal of methylene blue from water, *Polym. Bull*., 33(2019).
30. C. M. J. Hu, W. Sun, Z. Ma, et al., Graphene oxide-polyethylene glycol incorporated PVDF nanocomposite ultrafiltration membrane with enhanced hydrophilicity, permeability, and antifouling performance, *Chemosphere*., 253(2020), 126649.
31. C. Mbareck, Q. T. Nguyen, Study of polysulfone and polyacrylic acid (PSF/PAA) membranes morphology by kinetic method and scanning electronic microscopy, *Membr. Sci. Technol*., 4(2014), 36-41.
32. M. Jyothi, M. Padaki, R. G. Balakrishna, R.K. Pai, Synthesis and design of PSf/TiO_2 composite membranes for reduction of chromium (VI): Stability and reuse of the product and the process, *J. Mater. Res*., 29(2014), 1537-1545.
33. A. Chtaini, S. Touzara, C.O.S. 'Id E, M. Chamekh, M. Mabrouki, A. Kheribech, Development of Graphite-DNA Polymer Composites as Electrode for Methanol Fuel Cells, *J. Mater. Sci. Eng*., 6(2017) 6-9.
34. E. Makhado, S. Pandey, P.N. Nomngongo, J. Ramontja, Preparation and characterization of xanthan gum-cl-poly(acrylic acid)/o-MWCNTs hydrogel nanocomposite as highly effective re-usable adsorbent for removal of methylene blue from aqueous solutions, *J. Colloid Interface Sci*., 513(2018), 700–714.
35. J. He, Y. Song, J.P. Chen, Development of a novel biochar/PSF mixed matrix membrane and study of key parameters in treatment of copper and lead contaminated water, *Chemosphere*., 186(2017), 1033-1045.
36. C. Peyratout, E. Donath, L. Daehne, Electrostatic interactions of cationic dyes with negatively charged polyelectrolytes in aqueous solution, *J. Photochem. Photobio. A Chem*., 142(2001), 51-57.
37. R. Salehi, F. Dadashian, E. Ekrami, Acid Dyes Removal from Textile Wastewater Using Waste Cotton Activated Carbon: Kinetic, Isotherm, and thermodynamic studies, *Prog. Color Color. Coat*., 11(2018), 9-20.
38. M. I. Khan, L. Wu, A. N. Mondal, Z. Yao, L. Ge, T. Xu, Adsorption of methyl orange from aqueous solution on anion exchange membranes : Adsorption kinetics and equilibrium, *Membr. Water Treat*., 7(2016), 23-38.
39. E. A. Abdelrahman, R.M. Hegazey, R.E. El-azabawy, Efficient removal of methylene blue dye from aqueous media using Fe / Si , Cr / Si , Ni / Si , and Zn / Si amorphous novel adsorbents, *J. Mater. Res. Technol*., (2019), 1-13.
40. H. M. F. Freundlich, Over the adsorption in solution, *J. Phys. Chem*., 57(1906), 385-471.
41. M. A. Hubbe, S. Azizian, S. Douven, Implication of pseudo-second-order adsorption kinetics on cellulosic materials: a review, *Bioresources*., 14(2019), 7582-7626.
42. M. K. Purkait, D. S. Gusain, S. DasGupta, S. De, Adsorption behavior of chrysoidine dye on activated charcoal and its regeneration characteristics using different, *Sep. Sci. Technol*., 39(2004), 2419-2440.
43. M. K. Uddin, A. Nasar, Decolorization of basic dyes solution by utilizing fruit seed powder, *KSCE J. Civ. Eng*., 24(2020), 345-355.
44. J. Cheng, C. Zhan, J. Wu, Z. Cui, J. Si, Q. Wang, X. Peng, L. Turng, Highly efficient removal of methylene blue dye from an aqueous solution using cellulose acetate nanofibrous membranes modified by polydopamine, *ACS Omega*., 5(2020), 5389-5400.
45. S. S. Samandari, J. Heydaripour, Onion membrane: an efficient adsorbent for decoloring of wastewater, *J. Environ. Heal. Sci. Eng*., 32(2015), 78-89.
46. Bai, Lu, Jia, Lu, Yan, Zhaodong, Liu, Zhicheng, Liu, Yaqing, Plasma-etched electrospun nanofiber membrane as adsorbent for dye removal, *Chem. Eng. Res. Des*., 38(2018).
47. I. Langmuir, The constitution and fundamental properties of solids and liquids, *J. Am. Chem. Soc.,* 40(1918), 1361-1403.
48. O. Ferrandon, H. Bouane, M. Mazet, Contribution à l'étude de la validité de différents modèles, utilisés lors de l'adsorption de solutés sur charbon actif, *Rev. Sci. Eau.*, 8(1995), 183-200.

How to cite this article:

E. Cheikh S'Id, A. Kheribech, M. Degué, Z. Hatim, R. Chourak, C. M'Bareck, Removal of methylene blue from water by polyacrylonitrile-co-sodium methallylsulfonate copolymer (AN69) and polysulfone (PSf) synthetic membranes*., Prog. Color Colorants Coat*., 14 (2021), 89-100.